

The Denaturation Transition of DNA in Mixed Solvents

Boualem Hammouda* and David Worcester^{†‡}

*National Institute of Standards and Technology Center for Neutron Research, Gaithersburg, Maryland; [†]Cold Neutrons for Biology and Technology Project, Department of Physiology and Biophysics, University of California-Irvine, Irvine, California; and [‡]Biology Division, University of Missouri, Columbia, Missouri

ABSTRACT The helix-to-coil denaturation transition in DNA has been investigated in mixed solvents at high concentration using ultraviolet light absorption spectroscopy and small-angle neutron scattering. Two solvents have been used: water and ethylene glycol. The “melting” transition temperature was found to be 94°C for 4% mass fraction DNA/d-water and 38°C for 4% mass fraction DNA/d-ethylene glycol. The DNA melting transition temperature was found to vary linearly with the solvent fraction in the mixed solvents case. Deuterated solvents (d-water and d-ethylene glycol) were used to enhance the small-angle neutron scattering signal and 0.1M NaCl (or 0.0058 g/g mass fraction) salt concentration was added to screen charge interactions in all cases. DNA structural information was obtained by small-angle neutron scattering, including a correlation length characteristic of the inter-distance between the hydrogen-containing (desoxyribose sugar-amine base) groups. This correlation length was found to increase from 8.5 to 12.3 Å across the melting transition. Ethylene glycol and water mixed solvents were found to mix randomly in the solvation region in the helix phase, but nonideal solvent mixing was found in the melted coil phase. In the coil phase, solvent mixtures are more effective solvating agents than either of the individual solvents. Once melted, DNA coils behave like swollen water-soluble synthetic polymer chains.

INTRODUCTION

DNA is a biopolymer formed of backbone phosphates, linked to desoxyribose sugars and side group amine bases (1). The charged phosphate groups are hydrophilic, the desoxyribose sugar groups are mostly hydrophobic, and the amine bases contain both hydrophobic and hydrophilic groups. This is based on water binding ability as referenced below. DNA forms a helical structure which is stable because of the stacking of the amine bases and of the hydrogen bonding between them. The helix phase melts into disordered coils under various conditions including temperature increase.

Most research on DNA has been in aqueous media at low concentration (2–10). Crystallographic measurements give precise sizes for the DNA helical structure: 3.4 Å average distance between adjacent phosphates, 34 Å for the helix pitch, and 20 Å for the helix diameter (3). The ultraviolet (UV) absorption spectroscopy method (3,4) has proven valuable for the characterization of the helix-to-coil transition. Some investigations used non-aqueous solvents such as ethylene glycol (6,9). Other analytical methods such as NMR or infrared (IR) spectroscopy (8,10) have been used to estimate hydration properties. It was found for instance that a specific number of water molecules are bound to each DNA nucleotide (10) (5 molecules per amine basepair, 4 molecules per phosphate, and 2 molecules per desoxyribose sugar group). X-ray and neutron fiber diffraction yielded information about water hydration as well (11). In Fuller et al. (11), it is stated “challenges in developing alternatives to a water environ-

ment can be expected to be very severe”. This article reports a study of the ethylene glycol alternative.

The helix-to-coil melting transition in DNA has been the subject of a large number of investigations in the literature, among which are review articles (12–14). Cheng and Pettitt (13) contains a selected literature review of experimental and modeling efforts. Stability of the helix structure is governed by the amine base stacking and the base-pairing through hydrogen-bonding. Factors like temperature, DNA concentration, pH, salt concentration and solvent mixtures affect the helix-to-coil transition (13). The helix-to-coil transition occurs in transcription and replication of DNA, and is also a key aspect of the polymerase chain reaction in biotechnology.

METHODS AND MATERIALS

The focus of our investigations is on the characterization of the helix-to-coil denaturation transition of DNA (1) in ethylene glycol and (2) in water/ethylene glycol mixtures. Two measurement methods are used: UV light absorption spectroscopy to characterize the helix-to-coil melting temperature and small-angle neutron scattering (SANS) to monitor structural changes across the melting transition.

DNA from salmon testes of molecular weight 1.3×10^6 g/mol was purchased from Sigma and used at a mass fraction of 4% mass fraction in all cases. This DNA has 41.2% (number fraction) GC content. To screen charge interactions, 0.1M (or 0.0058 g/g mass fraction) concentration of NaCl salt was added in all cases.

The helix-to-coil denaturation transition in DNA (UV absorption spectroscopy)

The conventional method for characterizing the helix-to-coil melting transition in DNA is UV absorption spectroscopy. The 260-nm absorbance

Submitted March 23, 2006, and accepted for publication June 13, 2006.

Address reprint requests to Boualem Hammouda, E-mail: hammouda@nist.gov.

© 2006 by the Biophysical Society

0006-3495/06/09/2237/06 \$2.00

doi: 10.1529/biophysj.106.083691

is a strong and reliable indicator of amine base stacking (or unstacking). A Cary 50 instrument was used with a temperature control system. Absorbance from the 4% DNA mass fraction samples was so strong that sample thicknesses around 50 μm were used to avoid signal saturation (i.e., to keep the absorbance below 3).

Signals from 4% mass fraction DNA/d-water/0.1M NaCl and 4% mass fraction DNA/d-ethylene glycol/0.1M NaCl were measured. Deuterated solvents (d-water and d-ethylene glycol) were used to keep consistency with the SANS measurements to be described later. Fig. 1 shows the melting curves and transition temperatures in both cases. The transition temperature with the d-ethylene glycol solvent is conveniently located at $38^\circ\text{C} \pm 0.5^\circ\text{C}$, well below the transition temperature with the d-water solvent at $94^\circ\text{C} \pm 0.5^\circ\text{C}$. The melting curves are characterized by a sharp increase of the 260-nm absorption (referred to as “first temperature” in Fig. 1), then a leveling off (referred to as “second temperature”). The transition temperature is chosen halfway between these two temperatures.

UV absorption spectroscopy measurements were made on a series of samples containing various fractions of d-water/d-ethylene glycol. All samples contained 4% mass fraction DNA and 0.1M NaCl. Fig. 2 shows the variation of the helix-to-coil melting temperature with solvent content together with the two characteristic temperatures (the first and second temperatures that give an indication of the transition range). It is seen that the melting temperature follows an almost linear variation (with a slight curvature around 80% mass fraction d-ethylene glycol) and that the transition range is fairly uniform. The reported transition temperatures were obtained upon heating. This melting transition is partially reversible although with strong hysteresis. The monotonic linear variation is attributed to the fact that the transition was approached from the helix side whereby solvents mix randomly (ideal solvent mixing behavior).

The fact that the melting temperature shown in Fig. 2 decreases with d-ethylene glycol fraction points to the conclusion that the hydrophobic groups CD_2 in d-ethylene glycol play an important role in the melting transition. They help solvent molecules cross the hydrophobic zone of the deoxyribose sugar groups thereby loosening the helical structure (unstacking of the amine bases and breaking of the hydrogen bonds between these bases).

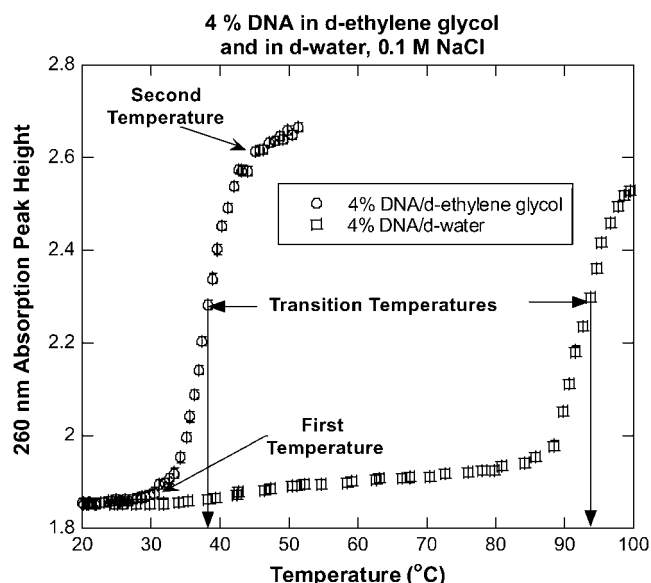


FIGURE 1 UV absorbance of the 260-nm line from 4% mass fraction DNA/d-ethylene glycol/0.1M NaCl and from 4% mass fraction DNA/d-water/0.1M NaCl and for a wide temperature range. The helix-to-coil denaturation transition is estimated to be $38 \pm 0.5^\circ\text{C}$ and $94 \pm 0.5^\circ\text{C}$, respectively. Vertical error bars are smaller than the symbols.

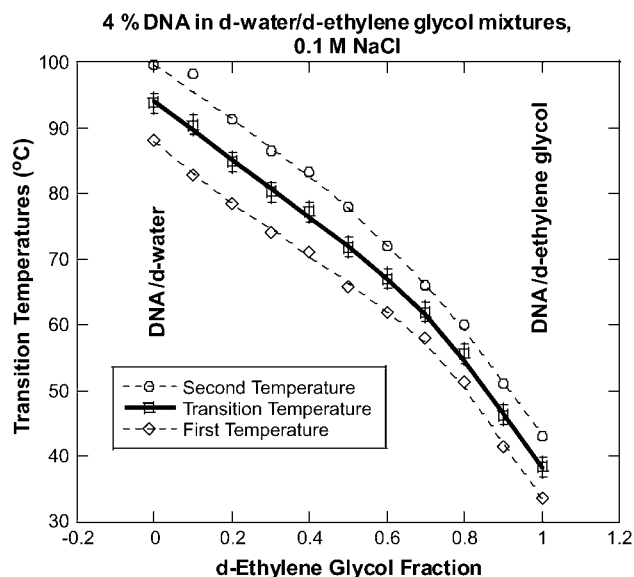


FIGURE 2 Variation of the denaturation melting temperature with increasing d-ethylene glycol fraction for 4% mass fraction DNA in mixtures of d-water/d-ethylene glycol. 0.1M NaCl salt was added in each case. The bottom left-half region corresponds to the helix phase and the top right-half region corresponds to the coil phase.

DNA dissolves in pure d-water or pure d-ethylene glycol. It also dissolves in 50% mass fraction d-water mixture with either one of the following solvents: d-methanol $\text{D}[\text{CD}(\text{OD})]\text{D}$, d-ethylene glycol $\text{D}[\text{CD}(\text{OD})]_2\text{D}$, or d-glycerol $\text{D}[\text{CD}(\text{OD})]_3\text{D}$. These three samples provide a convenient series whereby the number of $[\text{CD}(\text{OD})]$ groups in the solvent molecule is increased. For these three samples, the melting temperature increases from 63.1°C for 4% mass fraction DNA/d-water/d-methanol/0.1M NaCl to 71.8°C for 4% mass fraction DNA/d-water/d-ethylene glycol/0.1M NaCl to 78.5°C for 4% mass fraction DNA/d-water/d-glycerol/0.1M NaCl. This result shows that even though both the CD and the OD groups in the solvent molecule are increasing equally, the melting temperature increases. A possible reason for this is that the extra OD groups tighten the hydration layer around the phosphate groups thereby stabilizing the helix phase. The extra CD groups cannot counteract this driving force.

These observations point to the importance of hydrophilic interactions (around the phosphate groups) and hydrophobic interactions (around the deoxyribose sugar groups) in the melting transition. When in the helix form, DNA is acting as a “micellar” system. The ability of the solvent to cross the hydrophobic region controls the stability of the helix phase.

Helix-to-coil transition: simple model

Many models are available in the literature to describe the helix-to-coil transition. Efforts by Zimm (15,16) and Flory (17,18), using a configuration matrix method, presented predictions of the helix-to-coil transition temperature for the single strand and the double strand helical structures. The method summarized in Flory's book (18) is followed here because of its intrinsic simplicity and its analytical form. Consider single strands consisting of N residues in the dilute regime and assume that the helical structure consists of ν helical sequences separated by coil sequences. Defining N_H as the total number of helical residues and $N_C = N - N_H$ as the total number of coil residues, the relative helical fraction is $p_H = N_H/N$ and the relative fraction of helical sequences is $p_\sigma = \nu/N$. Introducing the enthalpy of melting of one helical residue as ΔH_m and the enthalpy of formation of one helical sequence as ΔH_σ , the associated partition function parameters are

defined as $s = \exp(\Delta H_m/RT)$ and $\sigma = \exp(\Delta H_\sigma/RT)$, where R is the molar gas constant and T is the absolute temperature. The solution for this configuration matrix approach was presented (18) in terms of the following eigenvalues:

$$\lambda_1 = \frac{(1+s) + \sqrt{(1-s)^2 + 4\sigma s}}{2}$$

$$\lambda_2 = \frac{(1+s) - \sqrt{(1-s)^2 + 4\sigma s}}{2}. \quad (1)$$

The relative fractions are then obtained as:

$$p_H = \frac{(\lambda_1 - 1)}{(\lambda_1 - \lambda_2)} \quad \text{and} \quad p_\sigma = \frac{(\lambda_1 - 1)(1 - \lambda_2)}{\lambda_1(\lambda_1 - \lambda_2)}. \quad (2)$$

The enthalpy parameter s is related to the temperature T as $s = 1 + \Delta H_m(T_m - T)/RTT_m$, where T_m is the melting temperature. A reasonable value for the enthalpy of melting $\Delta H_m = -6$ kcal/mol was used from the literature (19). The rescaled UV absorption data for the 4% DNA/0.1 M NaCl/d-ethylene glycol are plotted in Fig. 3 along with the model's best fit to the data corresponding to $\sigma = 0.0037$. This value implies ~ 29 helical sequences per 1000 residue at the melting transition point (at $T = T_m$) and an enthalpy of helical sequence formation of $\Delta H_\sigma = 3,463$ cal/mole. Zimm (16) had predicted a value between 1.5 and 3 kcal/mol.

Other more involved models are available for the prediction of the helix-to-coil melting transition (19–21). These are based on numerical solutions and will not be pursued here.

SANS data across the DNA melting transition

SANS is a valuable measurement method for investigating structural changes and phase transitions in macromolecular systems. The use of deuterated solvents enhances the neutron contrast and therefore the measured signal. This technique probes length scales from the near atomic scale (a few angstroms) to the near micrometer scale. Focus in these investigations was put on the local structure measured in the high- Q region. Q is the magnitude of the scattering vector; it is proportional to the scattering angle (at the small

angle approximation) and inversely proportional to characteristic inter-distances between scatterers within the sample.

The SANS technique uses a highly collimated monochromatic neutron beam incident on the sample. The scattered beam is detected by a position sensitive neutron area detector which records the scattering intensity for increasing scattering vector $Q \approx 2\pi\theta/\lambda$, where θ is the scattering angle and λ is the neutron wavelength. SANS measurements were performed at the NIST Center for Neutron Research (NG3 SANS instrument). Standard data collection and reduction methods were used to obtain scattering intensity $I(Q)$ on an absolute scale. Optimal sample thicknesses of 1 mm were used in all cases. A series of measurements were performed from a 4% mass fraction DNA/d-ethylene glycol/0.1M NaCl sample at temperatures ranging from 10°C to 80°C (at 5°C intervals). Fig. 4 shows a typical SANS spectrum at two temperatures; one below (25°C) and the other one above (50°C) the helix-to-coil transition temperature. The high- Q SANS signal is distinctively different in the two cases. The data show an abrupt decrease in the high- Q intensity for the helix phase but a gradual decrease for the coil phase.

SANS is sensitive to composition fluctuations in the sample. The helix structure is more compact and therefore characterized by a higher SANS intensity $I(Q)$. SANS intensities are therefore characteristically different in the helical and coil phases. The SANS intensity data were fit to the following functional form (22,23) that reproduces the main data features:

$$I(Q) = A/Q^n + C/[1 + (QL)^m] + B. \quad (3)$$

The term A/Q^n represents the low- Q network scattering part and the term $C/[1 + (QL)^m]$ represents the high- Q solvation part. B represents a Q -independent (mostly incoherent) background. The low- Q part represents scattering from a large gel network structure. As shown in Fig. 4, the low- Q part does not change much across the melting transition. Our focus here is on the high- Q signal exclusively. Nonlinear least-squares fits were performed on the SANS data to obtain the C , L , m , and B parameters.

Fig. 5 shows the variation of the “solvation intensity” (the fitted quantity C in Eq. 1) for increasing temperature. The intensity drop between 25°C and 40°C characterizes the helix melting transition. Lowering temperature shows that this transition is weakly reversible with substantial hysteresis. Further

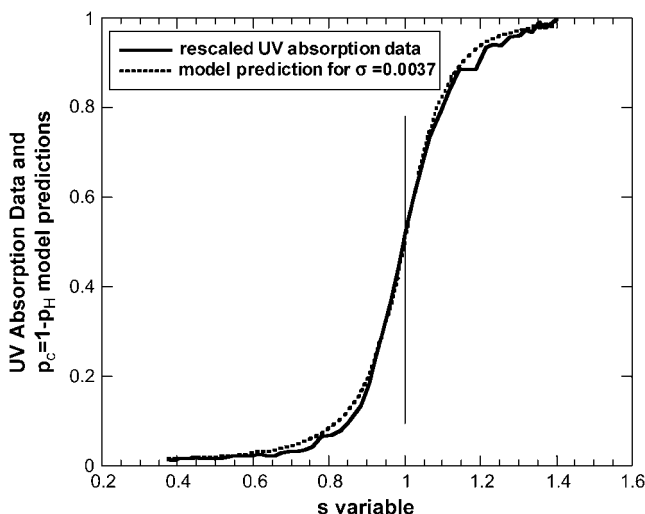


FIGURE 3 The UV absorption data for the 4% DNA/0.1 M NaCl/d-ethylene glycol sample across the helix-to-coil transition is compared to model prediction for the coil fraction $p_C = 1 - p_H$ with the best fit parameter $\sigma = 0.0037$. An enthalpy of melting of $\Delta H_m = -6$ kcal/mol has been used.

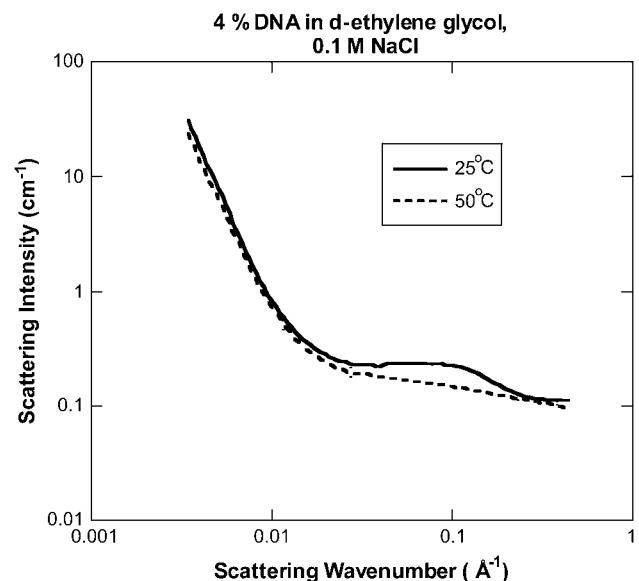


FIGURE 4 Small-angle neutron scattering from a 4% mass fraction DNA/d-ethylene glycol/0.1M NaCl sample measured at temperatures below (25°C) and above (50°C) the helix-to-coil melting temperature. The high- Q signal clearly shows structural change across the melting transition. Error bars are very small.

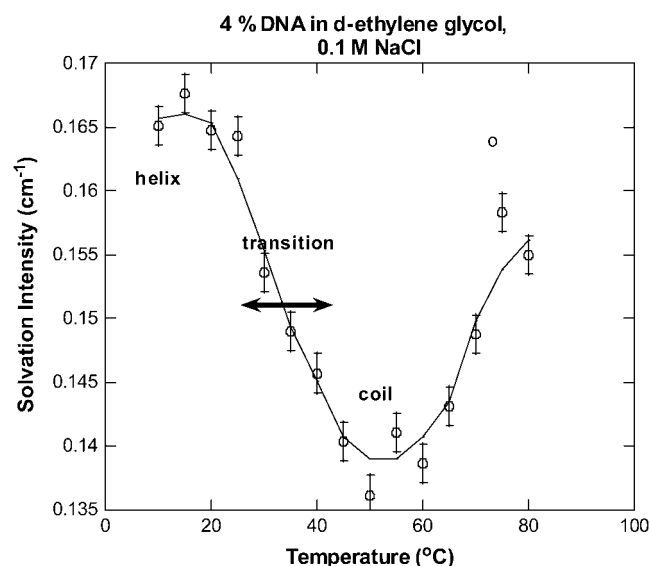


FIGURE 5 Variation of the SANS solvation intensity (the quantity C in Eq. 1) for increasing temperature for a 4% mass fraction DNA/d-ethylene glycol/0.1M NaCl sample. For temperatures beyond the melting transition, the solvation intensity increases. Error bars correspond to three standard deviations.

temperature increase beyond the melting transition increases the solvation intensity as shown in Fig. 5. This result is typical of water-soluble polymers and was observed for a 4% mass fraction poly(ethylene oxide)/d-water solution (22). In the case of PEO, the solvation intensity increased until a Lower Critical Solution Temperature (LCST) of 105.4°C was reached.

Fig. 6 summarizes the variation of the correlation length (the quantity L in Eq. 1) across the melting transition. Neutrons “see” hydrogen more than any other atoms. This correlation length represents a weighted-average interdistance between the hydrogen-containing (mostly sugar-amine base) groups. It is $\sim 8.5 \pm 0.2$ Å in the helix phase and increases to 12.3 ± 0.2 Å in the coil phase. In the helix phase the sugar-amine base groups are closer together than in the coil phase. This increase in L is due to the opening of the tight helix structure into a looser coil configuration. This correlation length is not a measure of the DNA radius (literature value of 10 Å in the helix phase). It is a measure of the correlations between hydrogen atoms. Raising the

temperature further in the coil phase increases the correlation length even more. A similar trend was also observed in PEO (22). The correlation length increases in the coil phase because correlations are transmitted more easily through the contour of flexible coils than they are through the stiff helical structures. In polymer coils, the correlation length is proportional to the entanglement length (average length between entanglement points along the polymer chain).

Fig. 7 represents the variation of the high- Q Porod exponent (the quantity m in Eq. 3). This exponent is seen to vary between values around 3.7 ± 0.1 in the helix phase to values close to 1.7 ± 0.1 in the coil phase. DNA helices are appearing like cylinders with fairly tight surfaces (Porod exponents close to 4) and DNA coils behave like polymer chains in good solvent conditions or in a fully swollen configuration (Porod exponent of $5/3 = 1.67$) (22).

It is noted that once the melting transition has taken place, DNA coils behave like water-soluble synthetic polymer chains.

Nonideal solvent mixing around DNA coils

SANS measurements were made for a series of 4% mass fraction DNA sample in mixed d-water/d-ethylene glycol solvent mixtures (with 0.1M NaCl salt added) at three temperatures: 1), at 25°C where all samples are in the helix phase (based on the UV data shown on Fig. 2); 2), at 50°C where most samples are in the helix phase and some are in the coil phase; and 3), at 75°C where most samples are in the coil phase. Fig. 8 shows variation of the solvation intensity (the quantity C in Eq. 1) with increasing d-ethylene glycol fraction and for the three measured temperatures. Linear variation is observed in the helix phase and parabolic variation is observed in the coil phase. In the helix phase, solvents mix randomly around the helical structures, whereas in the coil phase nonideal solvent mixing is observed. Similar results were obtained in the case of a series of 4% mass fraction poly(ethylene oxide) (or PEO) solutions in mixtures of d-water and d-ethylene glycol (B. Hammouda, unpublished data). When in the presence of hydrophobic and hydrophilic groups, mixed solvents tend to arrange themselves efficiently so as to minimize conformational “stress” around the polymer coils in the solvation shell. Solvent mixtures are better solvation agents than either of the individual solvents. This is manifested as a lower solvation intensity as shown in the parabola portions of the graphs in Fig. 8. The SANS technique cannot resolve the orientational conformations of the solvent molecules around the DNA coils. Such a task is very difficult for noncrystalline systems like the ones investigated here, but SANS can monitor chain conformation fluctuations reliably. Our results point to the fact that when in the coil state, DNA behaves like the simplest water-soluble polymer (PEO) despite its chemical complexity.

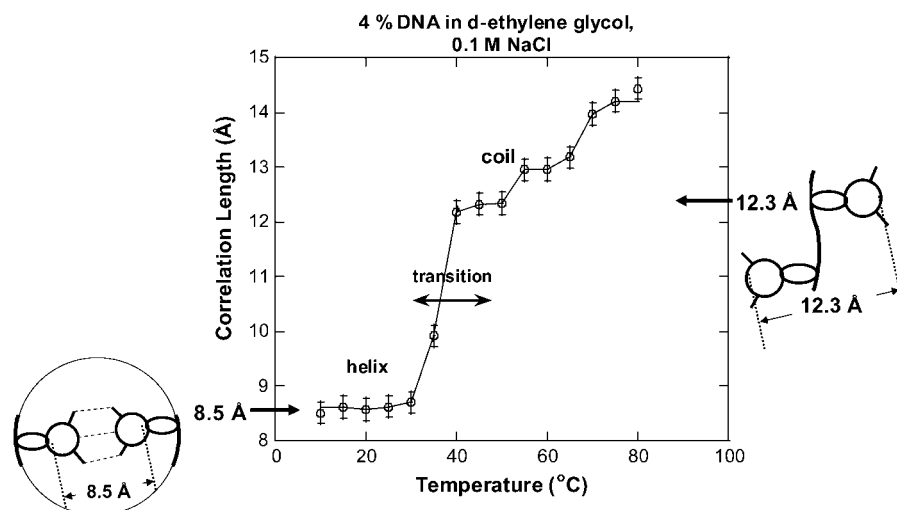


FIGURE 6 Variation of the correlation length (the quantity L in Eq. 1) for increasing temperature for a 4% mass fraction DNA/d-ethylene glycol/0.1M NaCl sample. A jump in the variation of the correlation length L across the helix-to-coil transition is observed (see the Figure insets). After melting, DNA coils swell with further temperature increase.

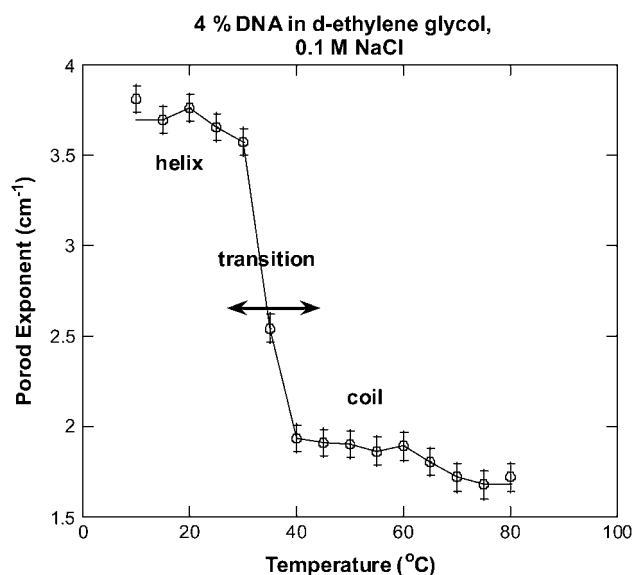


FIGURE 7 Variation of the high- Q Porod exponent (the quantity m in Eq. 1) for increasing temperature for a 4% mass fraction DNA/d-ethylene glycol/0.1M NaCl sample. This exponent varies from 3.7 (cylinder) to 1.7 (swollen coil).

DISCUSSION AND CONCLUSIONS

Our results show that the salmon DNA helical structures are less stable in d-ethylene glycol than in d-water which is seen

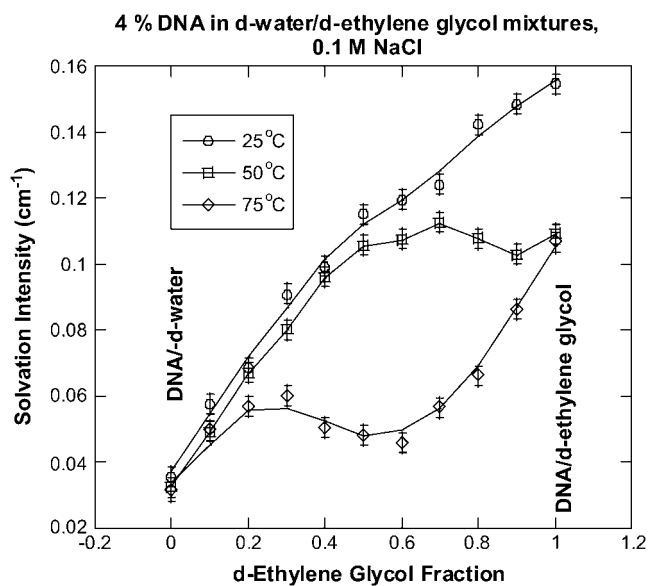


FIGURE 8 Variation of the SANS solvation intensity (the quantity C in Eq. 1) for increasing d-ethylene glycol fraction in a series of 4% mass fraction DNA samples in d-water/d-ethylene glycol solvent mixtures measured at three temperatures (25°C, 50°C, and 75°C). 0.1M NaCl salt was added in all cases. Ideal solvent mixing is observed around DNA helices (linear variation), whereas nonideal solvent mixing is observed around DNA coils (parabolic variation).

as a decrease of the helix-to-coil transition temperature. This conclusion is in agreement with an earlier report (9) for 21-mer DNA at low concentration. This is partly due to water's greater ability to form hydrogen bonds. Ethylene glycol's ability to form hydrogen bonds is lower because of the hydrophobic- D_2 groups. Ethylene glycol is the only nonaqueous solvent found to dissolve DNA in its pure form. Other solvents such as alcohols (for example ethanol) dissolve DNA only when they are mixed with water. Some of these solvents reported in the literature (9) are formamide, dimethyl sulfoxide, methanol, ethanol, and glycerol.

UV and SANS measurements have been conducted to characterize the helix-to-coil transition for 4% mass fraction DNA in d-water (94°C) and in d-ethylene glycol (38°C) with 0.1M NaCl salt content. Transition temperatures obtained from the two analytical methods are consistent. Measurements have also been made on DNA in mixtures of these two solvents over the entire mixing range. Linear variation of the transition temperature was found. The coil phase can be reached either through heating or by varying the d-water/d-ethylene glycol solvent content.

Structural information on the helix and coil phases has been obtained by SANS. Helices behave like cylinders with fairly tight surfaces. Coils are in a fully swollen configuration. A measured correlation length was found to increase from 8.5 Å to 12.3 Å across the DNA melting transition for the DNA/d-ethylene glycol/0.1M NaCl system. This correlation length is a characteristic interdistance between the hydrogen-containing (sugar-amine base) groups. In the helix phase, these groups are close together (inside the helix), whereas in the coil phase they are disordered side groups on the randomly distributed DNA coils. Beyond the melting transition, DNA coils behave like the simplest water-soluble polymer (PEO) chains. They swell with further temperature increase. A significance of these findings is that DNA with its complicated structure behaves like the simplest water soluble polymer when in the coil phase. The main significance is the substantial lowering of the helix-to-coil transition temperature when ethylene glycol is used. Ethylene glycol (prime ingredient in antifreeze) is a toxic poison and is of interest in biology research.

In the case of mixed solvents, it was found that solvent molecules mix randomly around the helical structures but not around the melted coils. In the coil phase, solvent mixtures were found to be more effective at solvating the polymer chains than any of the individual solvents.

Discussions with Ferenc Horkay from National Institutes of Health are greatly appreciated. The identification of commercial products does not imply endorsement by the National Institute of Standards and Technology.

This work is based upon activities supported in part by the National Science Foundation under agreement No. DMR-0454672 for the Center for High Resolution Neutron Scattering program and in part by the National Institutes of Health under grant No. 1 R01 RR14812 for the Cold Neutrons for Biology and Technology program.

REFERENCES

1. Becker, W. M., L. J. Kleinsmith, and J. Hardin. 1999. *World of the Cell*. Benjamin/Cummings Publishing, New York.
2. Van Holde, K. E., W. Curtis Johnson, and P. Shing Ho. 2006. *Principles of Physical Biochemistry*. Pearson Prentice Hall, New York.
3. Arnott, S., R. Chandrasekaran, D. L. Birdsall, A. G. W. Leslie, and R. L. Ratliff. 1980. Left-handed DNA helices. *Nature*. 283:743–745.
4. Rozners, E., and J. Moulder. 2004. Hydration of short DNA, RNA and 2-OMe oligonucleotides determined by osmotic stressing. *Nucleic Acids Research*. 32:248–254.
5. Muraoka, M., H. T. Miles, and F. B. Howard. 1980. Copolymers of adenylic and 2-aminoadenylic acids. Effect of progressive changes in hydrogen bonding and stacking on interaction with poly(uridylic acid). *Biochemistry*. 19:2429–2439.
6. Iwataki, T., S. Kidoaki, T. Sakaue, K. Yoshikawa, and S. Abramchuk. 2004. Competition between compaction of single chains and bundling of multiple chains in giant DNA molecules. *J. Chem. Phys.* 120:4004–4011.
7. Podgornik, R., H. H. Strey, D. C. Rau, and V. A. Parsegian. 1995. Watching molecules crowd: DNA double helices under osmotic stress. *Biophys. Chem.* 57:111–121.
8. Strzelecka, T. E., and R. L. Rill. 1990. A Na-23 NMR study of Na-DNA interactions in concentrated DNA solutions at low-supporting electrolyte concentration. *Biopolymers*. 30:803–814.
9. Bonner, G., and A. M. Klibanov. 2000. Structural stability of DNA in nonaqueous solvents. *Biotechnol. Bioeng.* 68:339–344.
10. Spink, C. H., and J. B. Chaires. 1999. Effects of hydration, ion release and excluded volume on the melting of triplex and duplex DNA. *Biochemistry*. 38:496–508.
11. Fuller, W., T. Forsyth, and A. Mahendrasingam. 2004. Water-DNA interactions as studied by x-ray and neutron fibre diffraction. *Philos. Trans. R. Soc. Lond. B Biol. Sci.* 359:1237–1247.
12. Gotoh, O. 1983. Prediction of melting profiles and local helix stability for sequenced DNA. *Adv. Biophys.* 16:1–52.
13. Cheng, Y. K., and B. M. Pettitt. 1992. Stabilities of double- and triple-strand helical nucleic acids. *Prog. Biophys. Mol. Biol.* 58:225–257.
14. Mergny, J. L., and L. Lacroix. 2003. Analysis of thermal melting curves. *Oligonucleotides*. 13: 515–537.
15. Zimm, B. H. and J. K. Bragg. 1959. Theory of the phase transition between helix and random coil in polypeptide chains. *J. Chem. Phys.* 31:526–535.
16. Zimm, B. H. 1960. Theory of melting of the helical form in double chains of the DNA type. *J. Chem. Phys.* 33:1349–1356.
17. Flory, P. J., and G. W. Miller. 1966. A general treatment of helix-coil equilibria in macromolecular systems. *J. Mol. Biol.* 15:284–297.
18. Flory, P. J. 1969. *Statistical Mechanics of Chain Molecules*, Chapter VII. Interscience Publishers, New York.
19. Dimitrov, R. A., and M. Zuker. 2004. Prediction of hybridization and melting for double-stranded nuclei acids. *Biophys. J.* 87: 215–226.
20. Applequist, J., and V. Damle. 1963. Theory of the effects of concentration and chain length on helix-coil equilibria in two-stranded nucleic acids. *J. Chem. Phys.* 39:2719–2721.
21. Applequist, J. 1969. Higher order phase transitions in two-stranded macromolecules. *J. Chem. Phys.* 50:600–609.
22. Hammouda, B., D. Ho, and S. Kline. 2004. Insight into clustering in poly(ethylene oxide) solutions. *Macromolecules*. 37:6932–6937.
23. Hammouda, B., F. Horkay, and M. Becker. 2005. Clustering and solvation in poly(acrylic acid) polyelectrolyte solutions. *Macromolecules*. 38:2019–2021.